

PHASE SYNCHRONIZATION and IMPROVEMENT OF CONTROLLABILITY OF THE NEAR WALL TURBULENCE

Sedat Tardu and Olivier Doche

Laboratoire des Ecoulements Géophysiques et Industriels (LEGI)

B.P. 53 X 38041 Grenoble, Cédex, France

Sedat.Tardu@hmg.inpg.fr

ABSTRACT

The effect of a spatially localized time-periodical perturbation on the controllability of the wall turbulence is analyzed. It is shown that the imposed unsteadiness with a frequency in the median production range doubles the controllability of turbulent drag. It is further observed that the spatially averaged turbulent wall shear is synchronized in time with the imposed perturbation waveform. This is related to the synchronization of the unstable periodic orbits present in the near wall turbulence in connection with the regeneration cycle of turbulence producing coherent structures.

INTRODUCTION

Intensive direct numerical simulation investigations conducted during the last decade have clearly shown that the optimal and suboptimal control of the near wall turbulence are plausible and that appreciable drag reduction can be achieved through either adaptive or non adaptive schemes. The literature on this topic is vast now and the reader may consult Bewley et al. (2001) for some recent ideas and developments. The major shortcoming of these methods is the necessity of a dense distribution of sensors (wall shear stress gauges) and actuators (micro blowing-suction jets) with a mesh size roughly equal to the viscous sublayer thickness to achieve significant drag reduction. Increasing the control mesh size decreases the efficiency of the control scheme. This not always well understood at a first glance. Indeed, the streamwise and spanwise scales of the coherent eddies near the wall are at least an order of magnitude larger than the required control space step. The quasi-streamwise vortices present in the buffer layer are about 300-500 wall units long and are separated by 100 wall units in the spanwise direction. They generate turbulent wall shear by stretching spanwise vorticity zones through ejections and sweeps. However their regeneration and locations are random in time and space and their capture and subsequent control decision require significantly smaller time and space scales. This poses technical feasibility problems of the sub-optimal strategies, despite the important progress achieved in micro-smart technologies nowadays. Investigations of somewhat simpler large-scale control methods are therefore still necessary.

The controllability can be easily defined and analyzed in some stability active control problems but is rather difficult to define in the absence of uncoupled modes as in the fully developed near wall turbulence. We will rather couple here the notion of controllability with that of predictability. It is without saying that rendering a process predictable (or deterministic-like) increases its degree of controllability. It is known that any unpredictable process $s[n]$ can be decomposed into $s[n] = s_\alpha[n] + s_\beta[n]$, where $s_\alpha[n]$ is a regular process and $s_\beta[n]$ is a predictable process orthogonal to $s_\alpha[n]$. This result is known as Wold's decomposition (Papoulis, 1985). In the case of the near wall turbulence $s_\beta[n]$ may be interpreted as the part due to the coherent structures, while $s_\alpha[n]$ is the incoherent part. The aim of a pseudo-robust control is then, to intervene locally in space somewhere at the wall to filter $s_\alpha[n]$, to accentuate $s_\beta[n]$ to control the flow more efficiently at further downstream locations.

The aim of this investigation is to check whether a localized imposed unsteadiness improves the controllability of the near wall turbulence or not. We consider a fully developed turbulent channel flow. The flow is locally forced through oscillating blowing by a slot as shown in Fig. 1. The sizes of the slot in wall units in the streamwise l_x^+ and spanwise l_z^+ directions are shown on this Fig.

Hereafter $()^+$ refers to quantities scaled by the inner variables namely the viscosity ν and the shear velocity

$$u_\tau = \sqrt{\frac{\tau}{\rho}}$$
 where τ is the wall shear stress and ρ is the

density. The time periodical blowing velocity is of the form $\langle v_0 \rangle = A \sin(2\pi ft)$. The imposed frequency is $f^+ = 0.018$ and it is in the median production range of the turbulent kinetic energy spectra $S(f)$, as shown schematically in

Fig.1. The time mean blowing velocity $v_0^+ = A^+ = 0.14$ is significantly small. There is no flow separation downstream the slot under these circumstances (Tardu, 2001).

DIRECT NUMERICAL SIMULATIONS

The degree of controllability is determined by applying adaptive suboptimal strategy downstream of the oscillating blowing zone as shown in Fig. 1. Contrarily to the optimal control whose aim is to laminarize the flow in a given time interval, the suboptimal strategy attempts to decrease at

each time step wall shear and the related the cost function. The latter is:

$$J(\phi) = \frac{k}{2\Gamma} \iint_w \phi^2 dS + \frac{1}{\Gamma} \iint_w \tau dS \quad (1)$$

where τ is the shear at the wall whose area is denoted by Γ , ϕ is the action at the wall in the form of pinpoint blowing/suction distribution and k is a constant. The first integral above is clearly the energy expended to achieve the drag reduction. The control problem consists of determining the optimum ϕ at each time step. The state equation is the Navier-Stokes equation:

$$\frac{\partial u_i}{\partial t} + \frac{\partial u_i u_j}{\partial x_j} = -\frac{\partial P}{\partial x_i} + \nu \frac{\partial^2 u_j}{\partial x_j^2} \quad (2)$$

where u_i and x_i are respectively the instantaneous local velocity and coordinates and P denotes the pressure. Mixed notations will be used here for convenience, i.e., the streamwise (x_1), wall normal (x_2) and spanwise (x_3) directions will also be denoted respectively by x , y and z together with the corresponding velocity components u (u_1), v (u_2) and w (u_3). The equation (1) is subject to the following boundary conditions at the wall, $x_2 = y = 0$:

$$\begin{aligned} u_1 &= 0 \\ u_2 &= \phi(x_1, x_3) \\ u_3 &= 0 \end{aligned} \quad (3)$$

The sensitivity of the cost function to the actuation modifications ϕ is measured through Fréchet derivatives as in classical non-linear control theory. The variation of a functional $\xi(\phi)$, denoted by $\tilde{\xi}(\phi, \tilde{\phi})$ is given by:

$$\tilde{\xi}(\phi, \tilde{\phi}) = \lim_{\varepsilon \rightarrow 0} \frac{\xi(\phi + \varepsilon \tilde{\phi}) - \xi(\phi)}{\varepsilon} = \iint_w \frac{F\xi(\phi)}{F\phi} \tilde{\phi} dS \quad (4)$$

where F stands for the Fréchet operator. In practice, the Navier-Stokes equation is discretized in time and space, and the resulting operators are transformed through the Fréchet operator. An adjoint problem is formulated and convenient choice of its boundary conditions allows to relate $\frac{DJ}{D\phi}$ to the fluctuating adjoint pressure field at the

wall. From $\frac{DJ}{D\phi}$ the actuation at the next time step $n+1$ is computed either by a conjugate gradient method

$$\phi^{n+1} = \phi^n - \alpha \left(\frac{DJ}{D\phi} \right)^n$$

or by a research of minima algorithm. To be brief, we followed the same procedure as in (Bewley et al., 1993) only with some subtle differences.

The Direct Numerical Simulations (DNS) are used to model the situation depicted in Fig.1. The code is of finite difference type combined with fractional time procedure. The non-linear terms are explicitly resolved by an Adams-Bashforth scheme. Periodical boundary conditions are used in the homogeneous streamwise and spanwise directions. The size of the computational domain is $(4\pi h \times 2h \times 1.33\pi h)$ in respectively the streamwise x , wall normal y and spanwise z directions, h standing for the channel half width. There are $(513 \times 129 \times 129)$ computational modes in (x, y, z) . Uniform and stretched coordinates are used in the streamwise, spanwise and wall normal directions. The first mesh from the wall is at 0.2

wall units. The mesh sizes in the x and z directions are respectively 4.5 and 5.5 $\ell_v = \frac{\nu}{u_\tau}$. The Reynolds number

based on the channel height and the centerline velocity is fixed at $Re = \frac{hU_c}{\nu} = 4200$ corresponding to

$$\begin{aligned} Re_\tau &= \frac{h u_\tau}{\nu} = 180. \\ \Delta t^+ &= \frac{\Delta t}{\ell_v} u_\tau = 0.1. \end{aligned}$$

RESULTS

The important quantity in term of turbulent drag control is the spatially averaged wall shear stress downstream of the localized unsteadiness. Thus the space-mean shear

$$[\tau](t) = \frac{1}{L_x^+ L_z^+} \int_0^{L_x^+} \int_0^{L_z^+} \tau dx^+ dz^+$$

is computed and its temporal evolution is analyzed. The zone wherein $[\tau]$ is determined extends up to $L_x^+ = 2000$ in the longitudinal direction downstream the blowing slot. The streamwise averaging extend is twice larger than the correlation length and an order of magnitude greater than the typical length of the coherent near wall vortices that is roughly 200 to 300 in wall units. The spanwise extend is that of the computational box, $L_z^+ = 753$. Fig. 2 shows the temporal evolution of $[\tau]$ for respectively under the effect of the localized blowing (LB) and suboptimal control (SC) alone, together with the dual control (DC), which is the combination of LB and SC. The spatially averaged $[\tau]$ is scaled with τ_s of the standard unmanipulated turbulent channel flow. It is seen that the drag downstream of the slot is reduced only by 3% under the effect of LB alone. LB indeed decreases the drag in an appreciable manner by roughly 30% in the zone $x^+ < 40$ immediately downstream the slot, but its effect relaxes rapidly at $x^+ \approx 400$ at which τ recovers its standard value τ_s (Tardu, 2001). The suboptimal control results in 8% of drag reduction. The drag reduction is doubled by dual control and reaches 16%. It has to be emphasized that the unsteady blowing is taken into account in the cost function under the DC strategy. The increase in the efficiency of the suboptimal control in DC is therefore not incidental. The localized unsteadiness increases the suboptimal controllability undeniably.

The second striking feature of the results presented in Fig.2 is the remarkably smooth temporal evolution of $[\tau]$ that regularly oscillates in the dual control case after the transient period $t^+ = 50$. The frequency of the oscillations in $[\tau]$ is exactly the frequency of the imposed unsteadiness. The amplitude of the oscillations is 5% and relatively small, but it has to be reminded that $[\tau]$ results from averaging in a large domain. Clearly $[\tau]$ is synchronized with the time periodical perturbation velocity $\langle v_0 \rangle$ under the effect of dual control.

The turbulence in general and the wall turbulence in particular can be seen as an infinite dimensional chaotic system. From this particular point of view, the imposed localized unsteadiness not only increases the controllability but also leads to a generalized synchronization of its spatiotemporal dynamics. The generalized synchronization

(GS) is included in the category of partial synchronization (PS) that refers to the situation wherein some state variables are synchronized but others are not (Boccaletti et al., 2002). The spatially averaged wall shear stress $[\tau]$ is the synchronized flow quantity here. Due to the physics of localized unsteady blowing in high imposed frequency regime $f^+ \geq 0.01$ (Tardu, 2001), wherein the unsteadiness is confined into the thin low buffer layer $y^+ < 10$ it is unexpected that the spatially averaged flow quantities in the external layer are synchronized. That is however unimportant in the context of drag reduction, since the control target here is $[\tau]$ which is clearly synchronized. We observed that the averaged turbulent wall shear stress intensity $[\tau']^2 = [\tau^2] - [\tau]^2$ exhibits also some periodicity in time and is correlated with the $[\tau]$ modulation. Fig. 3

shows the temporal evolution of $\frac{\sqrt{[\tau'^2]}}{\tau'_s}$ in the case of dual control where τ'_s is the turbulent wall shear stress intensity of the standard channel flow. The turbulent shear activity decreases up to 50% under essentially the effect of the suboptimal control. That has to be compared to the smaller 16% decrease in $[\tau]$ resulting in a pronounced disequilibrium of the wall turbulence. There is clearly a dominant frequency equal to that of the blowing velocity modulation in the $\sqrt{[\tau'^2]}$ evolution as it is seen in Fig.3.

The $\sqrt{[\tau'^2]}$ oscillations are weak but still correlated to $[\tau]$. Therefore, the spatially averaged state variables in the viscous sublayer are functionally related to $[\tau]$ and the process can thus be categorized as GS.

The strategy used here is conform to the original idea of (Ott et al., 1990) in the sense that the aimed performance is obtained by making only small time-dependent perturbations to the wall normal velocity system parameter. The periodic perturbation is local in space and the subsequent adaptive suboptimal scheme propagates its effect to a large spatial domain. Both techniques are used in chaos control (Boccaletti et al., 2000). Periodic parametric perturbations applied to low and high dimensional systems with imposed frequencies corresponding to rational multiples of the frequencies of the periodic orbits (UPO's) result in chaos synchronization (Mirus and Sprott, 1990). UPO's have recently been found in Couette turbulence and some control strategies inspired from chaos control methodology have been proposed (Kawahara et al., 2006). The periodic motion embedded in the Couette turbulence is related to the regeneration cycle of the near wall Reynolds shear stress producing eddies. A directly similar investigation does not exist in the case of fully developed turbulent channel flow. However it is strongly suspected that UPO's in channel flow are also presumably linked to the genesis of the near wall coherent vortices (Holmes et al., 1996; Hamilton et al., 1995; Waleffe, 2003). The imposed frequency $f^+ = 0.018$ used here is precisely the regeneration frequency (commonly called ejection frequency f_e^+) of the coherent vortices in the low buffer layer at $y^+ = 20$ where the turbulence production reaches its maximum (Tardu, 2002). The ejection frequency varies

continuously from $f_{e\min}^+ \approx 0.001$ at the wall to $f_{e\max}^+ \approx 0.03$ in the log-layer. Further computations we conducted have indeed shown that PS does no more occur for $f^+ \geq f_{e\max}^+$ strengthening the arguments presented here.

It has to be emphasized that the imposed perturbation is spatially local here, and the results are therefore more attractive from a feasibility point of view. The forcing is applied through boundary conditions contrarily to [Guan et al. (2004) wherein the streamwise velocity component is unidirectionally coupled with a target state in the whole flow domain. The adaptive suboptimal control applied downstream of the localized perturbation sorts out the UPO and leads to partial synchronization.

The dual and suboptimal controls are structurally different. Fig. 4 compares the wall shear stress and the associated coherent structures resulting from the suboptimal and dual control strategies. The SC suppresses drastically the quasi-streamwise vortices and the turbulent wall sheara stress intensity decreases in an important manner as discussed before. In the case of DC, however, there are comparatively more structures, yet the drag decrease is

twice larger. The ratio $\frac{\sqrt{[\tau'^2]}}{[\tau]}$ is respectively 0.20 and

0.25 in the SC and DC cases to be compared with 0.37 of the non-manipulated flow. Thus, both configurations lead to a turbulence state, which is strongly in disequilibrium, the degree of which is only slightly smaller in dual control. One may conclude that the DC plays the role of equilibrium regulator with more or less success.

CONCLUSION

In conclusion we have shown that adding an external frequency to the wall turbulence in the range of the regeneration cycle spectrum increases the suboptimal controllability of the turbulent drag. The second effect of the imposed unsteadiness is the coupling with preexisting UPO's leading to a controlled wall shear stress that smoothly oscillates with appreciably less turbulent activity. The present strategy may be applied to achieve active control with a significantly less density of the wall controllers using several local oscillators recovering the entire broadband spectra of the wall turbulence in the production range.

REFERENCES

- Bewley T., Choi H., Temam, Moin P., 1993, Annual Research Briefs, Center of Turbulence Research, Stanford Un., pp. 3-14.
- Bewley T., Moin P., Temam R., 2001, J. Fluid Mech., **447**, 179.
- Boccaletti S., Grebogi C., Lai Y.C., Mancini H., Maza, D., 2000, Phys. Rep., **329**, 103.
- Boccaletti S., Kurths J., Osipov G., Valladeres D.L., Zhou C.S., 2002, Phys. Rep., **366**, 1.
- Guan S., Wie G.W., Lai C.H., Phys. Rev. E, **69**, 066214, 2004.
- Hamilton J.M., Kim J., Waleffe F., 1995, J. Fluid Mech., **287**, 317.

Holmes P., Lumley J.L., Berkooz G., 1996, *Turbulence, Coherent Structures, Dynamical Systems and Symmetry*, Cambridge Un. Press, Cambridge.

Kawahara G., Kida S., van Veen L., 2006, *Nonlinear Processes in Geophysics*, **13**, 499.

Mirus K.A., Sprott J.C., 1999, *Phys. Rev. E*, **59** (5), 5313.

Ott E., Grebogi C., Yorke Y.A., 1990, *Phys. Rev. Lett.*, **64**, 1196.

Papoulis A., 1985, *IEEE Trans. Acoustics, Speech and Signal Processing*, **ASSP-33**, 933.

Tardu S., 2001, *J. Fluid Mech.*, **43**, 217.

Tardu S., *Exp. in Fluids*, **33**, 640, 2002.

Waleffe F., *Phys. Fluids*, **15**, 1517, 2003.

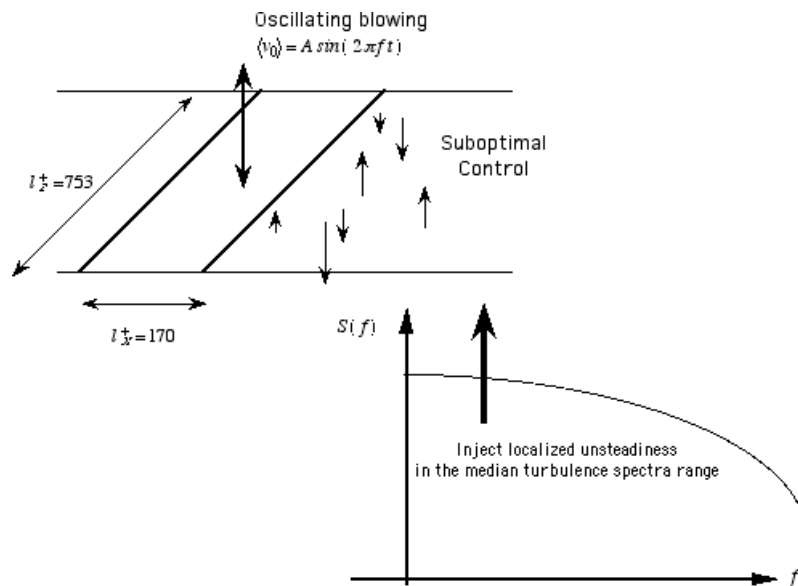


Figure 1 Wall turbulent dual drag control strategy. The flow is perturbed locally by oscillating blowing through a localized slot. The suboptimal adaptive control is applied downstream (top). The frequency of the localized unsteady perturbation is in the median range of the turbulence spectra (below).

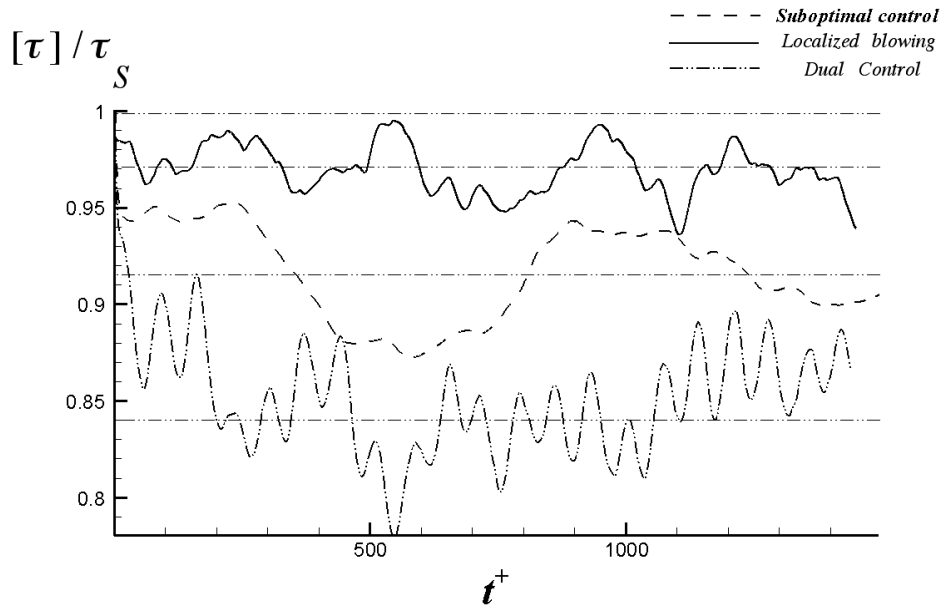


Figure 2 In situ comparison of the temporal evolution of the spatially averaged wall shear stress under respectively the effect of the localized blowing and suboptimal control alone and the dual control that is their combination.

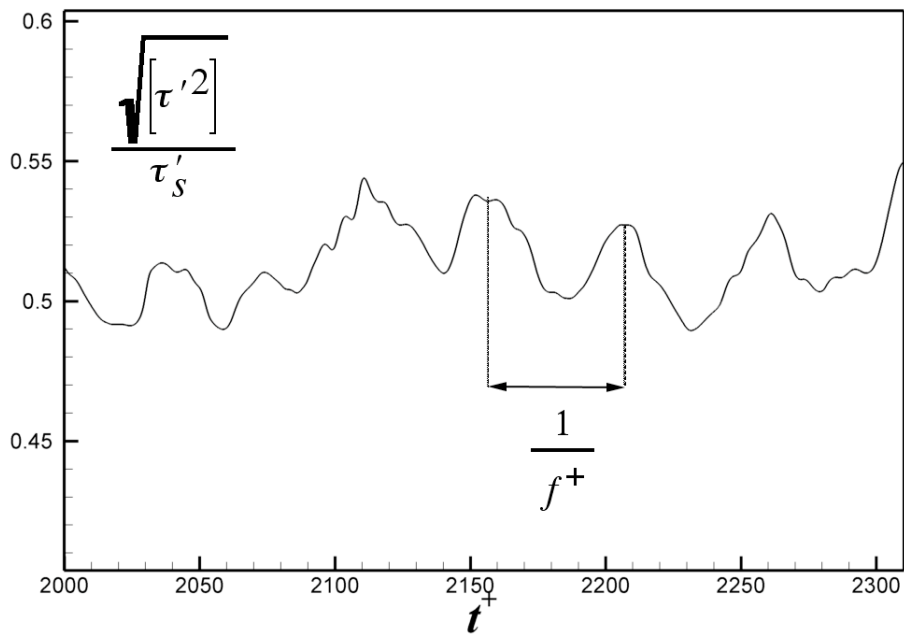
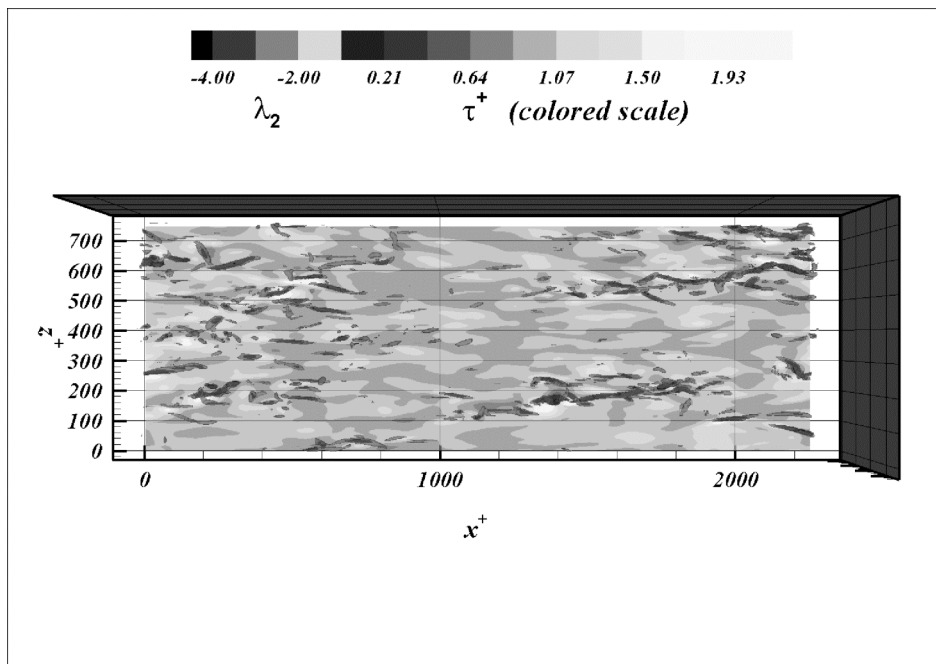


Figure 3 Temporal evolution of the space-averaged turbulent wall shear stress intensity in the case of dual control. Relatively weak oscillations synchronized with the imposed unsteadiness frequency f^+ are clearly visible.

a-



b-

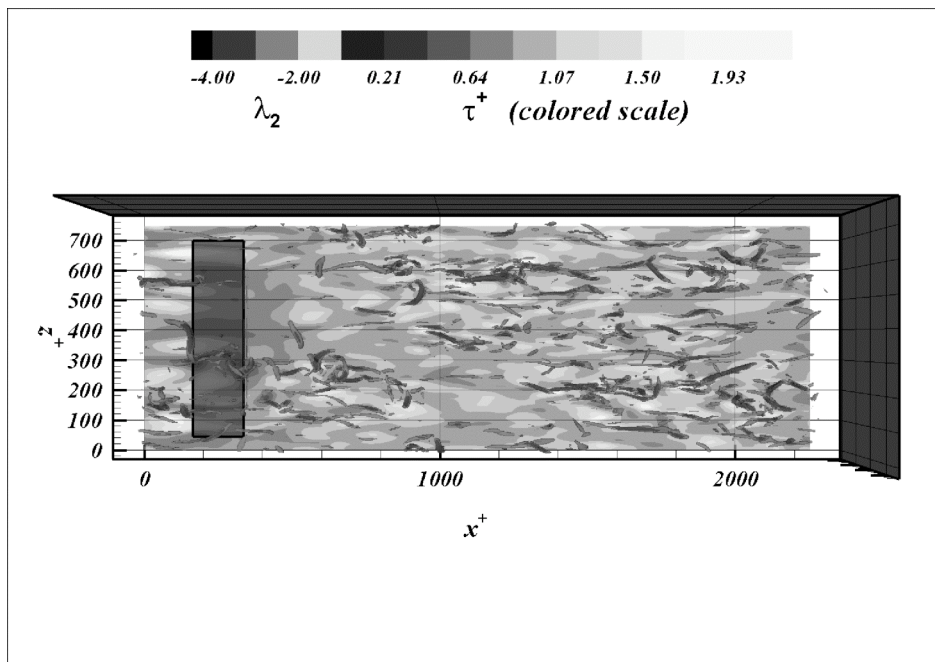


Figure 4 The shear stress and wall coherent structures detected by λ_2 in the case of suboptimal (a) and dual (b) control.